Sebastião Romero Franco; Leandro Farina

Shoaling of nonlinear steady waves: maximum height and angle of breaking

In: Jan Brandts and Sergey Korotov and Michal Křížek and Karel Segeth and Jakub Šístek and Tomáš Vejchodský (eds.): Application of Mathematics 2015, In honor of the birthday anniversaries of Ivo Babuška (90), Milan Práger (85), and Emil Vitásek (85), Proceedings. Prague, November 18-21, 2015. Institute of Mathematics CAS, Prague, 2015. pp. 45–62.

Persistent URL: http://dml.cz/dmlcz/702964

*Conference Applications of Mathematics 2015, in honor of the birthday anniversaries of Ivo Babuška (90), Milan Práger (85), and Emil Vitásek (85)*
J. Brandts, S. Korotov, M. Křížek, K. Segeth, J. Šístek, T. Vejchodský (Eds.)
Institute of Mathematics CAS, Prague 2015

# SHOALING OF NONLINEAR STEADY WAVES: MAXIMUM HEIGHT AND ANGLE OF BREAKING

Sebastião Romero Franco[1], Leandro Farina[2,3]

[1] Departamento de Matemática, Universidade Estadual do Centro-Oeste,
Irati, PR, Brazil
romero@irati.unicentro.br
[2]Instituto de Matemática, Universidade Federal do Rio Grande do Sul,
Porto Alegre, RS, 91509-900, Brazil
farina@mat.ufrgs.br
[3]BCAM - Basque Center for Applied Mathematics,
Mazarredo 14, 48009 Bilbao, Basque Country, Spain
lfarina@bcamath.org

**Abstract:** A Fourier approximation method is used for modeling and simulation of fully nonlinear steady waves. The set of resulting nonlinear equations are solved by Newton's method. The shoaling of waves is simulated based on comparisons with experimental data. The wave heights and the angles of breaking are analysed until the limit of inadequacy of the numerical method. The results appear quite close to those criteria predicted by the theory of completely nonlinear surface waves and contribute to provide information on the study of the relationship between computational modeling and the theory of steady waves.

**Keywords:** nonlinear water waves, steady waves, wave shoaling, angle of wave breaking, maximum wave height, spectral method

**MSC:** 74J30, 76B15, 74S25

## 1. Introduction

Waves in water are natural phenomena which have been extensively studied. The knowledge about its properties is of fundamental importance in several socio-economical activities, such as coastal environment protection, industrial activities in deep waters, where an analysis of the impact and force of waves is of extreme importance. Other not less important activities are applications to sailing, sediment transport prediction and conversion of waves energy into electrical energy.

The study of wave shoaling and breaking has a deserved remarkable place in this context, given that the energy of waves is intrinsically associated to the wave's

height. Experimental, analytical and computational methods have been used for investigation of these phenomena. A certain amount of experimental data about wave shoaling is known. Among these, the field data in [11] and the laboratory measurements in [6] are classical and used for validation of numerical methods. More recently Tsai et al. [17] examined criteria used in wave breaking via experimental results. In their work, steeper bottoms have been studied.

From the analytical and computational points of view, the paper by Rienecker and Fenton [14] has been one of the first work to propose a method for the simulation of steady completely nonlinear water waves. Denominated as Fourier methods, this technique does not assume analytical approximations and the solution of the nonlinear equations for the dynamics of waves is expressed by a Fourier series. The nonlinear equations obtained are resolved numerically by Newton's method. A great number of subsequent papers propose improvements and extension of Fourier methods to the study of nonlinear free surface waves. Gimenez-Curto and Corniero Lera [10] present procedures to reduce the computation time of Fourier methods for very long waves. Assuming Fourier's expansions of superior orders and including nonlinear interactions of arbitrary order, Dommermuth and Yue [3, 18] expanded Fourier methods via a spectral method of superior order and calculated the evolution of nonlinear waves in several cases, including the interaction between two waves.

Approaches with analytical approximations for the calculation of nonlinear waves have also been used [19]. Freilich and Guza [9] use variants of Boussinesq equations to study the shoaling of waves. Fenton [7] deduced expressions of fifth order based on Stoke's theory and presented numerical results, comparing them to experimental data. In this same context, Pihl et. al. [13] examined the shoaling of waves described by an approximation of sixth order in the presence of a current.

For studies of nonlinear waves dynamics with a more computational emphasis, we cite Drimer and Agnon [4], which uses the boundary element method and the work of Bingham and Zhang [1] for an approach of the problem through finite differences of higher order. Finally, Ducrozet et. al. [5] make a comparative study of two fast methods for the problem of nonlinear surface waves: the higher order spectral method and the higher order method of finite differences.

In this paper, we solved the problem of steady completely nonlinear surface waves by Fourier methods combined with Newton's method [2]. No analytical approximation is done and we assume that in a bottom with declivity, waves in any depth behave as if the bottom were horizontal. The approximation by Fourier series showed to be a very powerful tool since it allows the direct calculation of accurate solutions, even for high waves and for every wavelength, except for a soliton's limit. We explored this characteristics to study with a certain level of detail, the phenomenon of wave shoaling.

The mathematical model and the non-dimensionalisation are presented with details in section 2. The approximation used for nonlinear steady waves is described in section 3, where we also present the computational approach. On section 4, the additional modeling and the method to examine the shoaling of waves are examined. In

subsection 5.1, the numerical results obtained are compared with experimental data. The maximum height and angle of wave breaking are examined computationally in subsections 5.2 and 5.3, respectively. Final conclusions are given in section 6.

## 2. Mathematical model

The mathematical description of the propagation of gravity waves on the water surface usually requires some assumptions about the water properties and the motion performed by it. Thus, we consider a homogeneous, incompressible fluid with non-rotational motion, where the main restoring force is due to the gravitational acceleration. Additionally, the viscosity and the surface tension are neglected. Moreover, we will not consider wind forcing.

We consider two-dimensional steady waves in water of finite depth and formulate the problem in terms of the stream function $\psi$. In what follows, we will use the same framework as in [14].

We will use symbol $*$ will denote dimensional variables and all variables are non-dimensionalised with respect to the acceleration of gravity $g^*$, and to the average depth, $\overline{\eta}^*$. Thus, consider the changes of variables $x = \frac{x^*}{\overline{\eta}^*}$, $y = \frac{y^*}{\overline{\eta}^*}$, $\eta = \frac{\eta^*}{\overline{\eta}^*}$, $\psi = \frac{\psi^*}{\sqrt{g^*\overline{\eta}^{*3}}}$, $Q = \frac{Q^*}{\sqrt{g^*\overline{\eta}^{*3}}}$, $R = \frac{R^*}{g^*\overline{\eta}^*}$. The spatial coordinates $x$ and $y$ indicate the horizontal and vertical direction with the origin of the Cartesian system lying at the water bottom. Here, $\eta$ is the water surface, $\psi$ is the stream function, $Q$ is the volumetric flow rate per unit wavelength normal to the plane $xy$ and $R$ is the total energy of the system.

Other non-dimensional variables relevant to the problem are the wave velocity $c = \frac{c^*}{\sqrt{g^*\overline{\eta}^*}}$, the wavenumber $k$ is defined by $k = k^*\overline{\eta}^* = \frac{2\pi}{\lambda^*}\overline{\eta}^*$, where $\lambda^*$ is the wavelength, the wave period is given by $\tau = \tau^*\sqrt{\frac{g^*}{\overline{\eta}^*}}$, and the so called arbitrary reference level $D$, is non-dimensionalised by $D = \frac{D^*}{\overline{\eta}^*}$.

We denote by $(u, v)$ the components of the velocity vector $\mathbf{u}$ and the stream function $\psi$ is defined such that $u = \frac{\partial\psi}{\partial y}$ and $v = -\frac{\partial\psi}{\partial x}$. $\psi(x, y)$ satisfies Laplace's equation

$$\frac{\partial^2\psi}{\partial x^2} + \frac{\partial^2\psi}{\partial y^2} = 0 \qquad \text{in } \ 0 < y < \eta(x). \tag{1}$$

The boundary conditions that must be satisfied by the stream function are

$$\psi(x, 0) = 0, \tag{2}$$

at the origin (background) and

$$\psi(x, \eta(x)) = -Q, \tag{3}$$

on the free surface $y = \eta(x)$.

In equation (3), it is assumed that water flow of moving from right to left is in the negative direction. On the free surface, the pressure is constant so that Bernoulli's equation gives:

$$\frac{1}{2}\left[\left(\frac{\partial\psi}{\partial x}\right)^2+\left(\frac{\partial\psi}{\partial y}\right)^2\right]+\eta=R. \tag{4}$$

The boundary conditions involving the wave periodicity are given by:

$$\lambda=\frac{2\pi}{k}, \tag{5}$$

and

$$\lambda=c\tau. \tag{6}$$

Next we define the contours of conditions, the condition of periodicity and some additional equations involving wave height, volume flow and wave speed, it is possible to obtain a closed system of variables that can be solved by Newton's method. We will describe, in the next section, how to to accomplish this, essentially by expanding the stream function $\psi$, in Fourier series.

## 3. Approximation of fully nonlinear steady waves

We present now the problem of fully nonlinear steady waves. The approximation of the solution is obtained by a spectral method combined with Newton's method [2, 14].

We expand $\psi(x,y)$ as

$$\psi(x,y)=B_0y+\sum_{j=1}^{N}B_j\frac{\sinh jky}{\cosh jkD}\cos jkx \tag{7}$$

for the Fourier coefficients $B_j$. This representation of the stream function assumes symmetry about the wave crest. The description below, in this section, is essentially the one given in [14]. We present some of the details here for completeness.

Note that the above expansion satisfies the Laplace's equation (1) and the boundary condition (2). The boundary condition (3) requires that

$$B_0\eta+\sum_{j=1}^{N}B_j\frac{\sinh jk\eta}{\cosh jkD}\cos jkx=-Q, \tag{8}$$

and the equation (4) takes the form

$$\frac{1}{2}\left[k\sum_{j=1}^{N}jB_j\frac{\sinh jk\eta}{\cosh jkD}\ \sin jkx\right]^2+\frac{1}{2}\left[B_0+k\sum_{j=1}^{N}jB_j\frac{\cosh jk\eta}{\cosh jkD}\ \cos jkx\right]^2+\eta=R, \tag{9}$$

for all $x$.

In these approximations, we observe that the arguments of $\sinh jk\eta$, $\cosh jk\eta$ and $\cosh jkD$ grow up rapidly with $j$. To avoid instability and numerical errors in the divisions in (9), we use the approximation

$$\frac{\cosh jk\eta}{\cosh jkD} \sim \frac{\sinh jk\eta}{\cosh jkD} \sim \exp\left[jk(\eta - D)\right], \tag{10}$$

for sufficiently large values of $j$.

The choice of an appropriate value for the parameter $D$ is important. We will adopt the non-dimensional value $D = 1$, suggested by Rienecker & Fenton [14], which corresponds to a value of relative water depth and characterises a regime of of water intermediate.

We will now impose equations (8) and (9) on $2N$ collocation points over one wavelength. This allows a discretisation of the problem. By symmetry, we can work with only $N+1$ points from the wave crest to the trough. Thus, we use the discretization $x_m = \frac{m\lambda}{2N}, \quad m = 0, 1, \ldots, N$. From $\lambda = \frac{2\pi}{k}$ it follows that $kx_m = \frac{m\pi}{N}$. Moreover, we abbreviate the notation of $\eta(x_m), u(x_m, y_m)$ e $v(x_m, y_m)$ to $\eta_m, u_m$ and $v_m$. Thus, from (8) and (9), we have:

$$B_0\eta_m + \sum_{j=1}^{N} B_j \frac{\sinh jk\eta_m}{\cosh jkD} \cos\left(\frac{jm\pi}{N}\right) + Q = 0, \tag{11}$$

$$\frac{1}{2}u_m^2 + \frac{1}{2}v_m^2 + \eta_m - R = 0, \tag{12}$$

for $m = 0, 1, \ldots, N$, where

$$u_m = B_0 + k\sum_{j=1}^{N} jB_j \frac{\cosh jk\eta_m}{\cosh jkD} \cos\left(\frac{jm\pi}{N}\right),$$

$$v_m = k\sum_{j=1}^{N} jB_j \frac{\sinh jk\eta_m}{\cosh jkD} \sin\left(\frac{jm\pi}{N}\right).$$

We now have $2N+2$ nonlinear equations. However, these involve $2N+5$ variables, which are $\eta_j, B_j, (j = 0, 1, \ldots, N)$, $k, Q$ and $R$. Thus, in principle, we need three further equations.

As the mean non-dimensionalised wave height is unity, we can write

$$\int_S \eta \, dS = 1, \tag{13}$$

where $S$ is the horizontal distance from the crest to the trough of the wave. Discretisation $x_0$ and $x_N$ represent the abscissas of these extremities and using the trapezoidal rule in (13), we have

$$\frac{1}{2N}\left[\eta_0 + \eta_N + 2\sum_{j=1}^{N-1} \eta_j\right] - 1 = 0. \tag{14}$$

In certain situations can solve the problem of nonlinear waves for prescribed values of the height $H$ and the wave period $\tau$. The height $H$ is merely the difference between the elevation of the crest $\eta_0$ and the height of the wave trough $\eta_N$. Hence,

$$\eta_0 - \eta_N - H = 0. \tag{15}$$

By combining equations (5) and (6), which involve the wave period, we have,

$$kc\tau - 2\pi = 0. \tag{16}$$

We obtained then, from (14)– (16), three new equations. We introduced, however, a new variable to the system; the wave velocity $c$. Therefore, let us analyse in more detail this quantity.

Let $c_E$ the Eulerian mean velocity $c_E$ of fluid. For steady waves, we have the relation [14]

$$c - c_E + B_0 = 0. \tag{17}$$

Alternatively, one can consider the drift velocity $c_s$ of the fluid particle, which is the mass transport velocity. In steady wave regime, with unit mean depth, volume flow $Q$ is equal to the mean velocity by which the fluid particle moves. Therefore, the speed of mass transport can be given by

$$c - c_s - Q = 0. \tag{18}$$

Finally, the $2N + 6$ equations (11), (12),(14)–(16), (17) or (18) form a closed system for the variables $(\eta_j, B_j (j = 0, 1, \ldots, N), k, Q, R, c)$.

## 4. Wave shoaling

The shoaling of waves occurs when they propagate in intermediary waters in a variable depth zone, gradually decreasing. In this study, it is assumed that the changes in depth occur in a smooth way. Thus, it can be assumed that the wave does not reflect and can adapt to the new depth. Due to energy conservation, when the group velocity, $C_g$, decreases, the wave tends to increase its height, or to shoal, until the subsequent wave break.

By using the wave refraction theory, it can be shown that the wave period is also constant during the process of shoaling. This follows from the conservation of crests for steady waves.

The phenomenon of incident waves shoaling on a coastal region has been well approximated by Rienecker& Fenton [14], assuming that if the bottom's inclination is less than $4,5^\circ$ the wave acts as if it is steady and with a constant local depth. Employing this hypothesis, a simple approximation neglects the dissipation by friction with the bottom and assumes that the wave period and the energy flux remain constant from a depth to another. That is, we assume that the conservation of crests occurs and there is no reflection of energy with decreasing of depth.

### 4.1. Method

To describe the shoaling of waves, due to the reduction of depth, the system of equations presented in section 3 must be extended to include the additional variables; the wave height $H$ and the average flux of energy $F$, of which the non-dimensional value can be written as [14]:

$$F = \frac{1}{2}c^3 - \frac{3}{2}c^2Q + c\left(2R - 1 - \frac{1}{2}QB_0 - \overline{\eta^2}\right) - Q(R-1), \tag{19}$$

where

$$\overline{\eta^2} = \frac{1}{2N}\left[\eta_0^2 + \eta_N^2 + 2\sum_{j=1}^{N-1}\eta_j^2\right].$$

The solution of the system from the starting depth provides the flux of energy according to equation (19). We will model the shoaling of waves by using a discrete and finite number of depths. For successive depths, the period and the flux of energy will be preserved, while the wave height $H$ will be the variable of the problem. Thus, we must include in the system, additional equations to specify the wave height for the starting depth and the flux of energy for subsequent depths.

The additional equations are

$$f_{2N+7} = \frac{1}{2}c^3 - \frac{3}{2}c^2Q + c\left(2R - 1 - \frac{1}{2}QB_0 - \overline{\eta^2}\right) - Q(R-1) - F = 0$$

and

$$\begin{aligned} f_{2N+8} &= H - \frac{H_0^*}{\overline{\eta}_0^*} = 0 \quad \text{for the initial depth, and} \\ f_{2N+8} &= F - F_0 = 0 \quad \text{for the subsequent depths,} \end{aligned}$$

where $F_0$ is the non-dimensional energy flux. We use Newton's method to solve the resulting discrete system.

An initial estimate for the energy flux is given as a function of the other variables. From Stokes approximation, we have

$$F = \frac{\pi}{8}\frac{c^2H^2}{\tau}\frac{\sinh k\cosh k + k}{\sinh^2 k}.$$

This estimate is necessary only for the first depth. Subsequently, for small changes in the depth, the following solution can be used as a good starting approximation for the problem, provided that the change in depth is calculated in the new non-dimensionalisation.

Suppose that the sub-index 1 is the solution for a certain depth and sub-index 2, the starting approximation of the next depth. Thus, the change of depth occurs as follows, $\overline{\eta}_2^* = \overline{\eta}_1^* \cdot r$. That is, $r = \overline{\eta}_2^*/\overline{\eta}_1^*$ is the ratio between the successive depths.

To obtain a satisfactory starting estimation of the variables to be used in the new depth, we assume the change in depths to be smooth. With this, we neglect the reflection of waves and we can use the last solution obtained as a good starting approximation for the next depth, as long as it is non-dimensionalised according to the new depth. That is,

$$H_2 = \frac{H_2^*}{\overline{\eta}_2^*} = \frac{H_1^*}{\overline{\eta}_2^*} = \frac{H_1\overline{\eta}_1^*}{\overline{\eta}_2^*} \implies H_2 = \frac{H_1}{r},$$

$$c_2 = \frac{c_2^*}{(g\overline{\eta}_2^*)^{\frac{1}{2}}} = \frac{c_1^*}{(g\overline{\eta}_2^*)^{\frac{1}{2}}} = \frac{c_1\,(g\overline{\eta}_1^*)^{\frac{1}{2}}}{(g\overline{\eta}_2^*)^{\frac{1}{2}}} \implies c_2 = \frac{c_1}{r^{\frac{1}{2}}},$$

$$k_2 = k_2^*\overline{\eta}_2^* = k_1^*\overline{\eta}_2^* = \frac{k_1}{\overline{\eta}_1^*}\overline{\eta}_2^* \implies k_2 = k_1 r,$$

$$Q_2 = \frac{Q_2^*}{[g(\overline{\eta}_2^*)^3]^{\frac{1}{2}}} = \frac{Q_1^*}{[g(\overline{\eta}_2^*)^3]^{\frac{1}{2}}} = \frac{Q_1\,[g(\overline{\eta}_1^*)^3]^{\frac{1}{2}}}{[g(\overline{\eta}_2^*)^3]^{\frac{1}{2}}} \implies Q_2 = \frac{Q_1}{r^{\frac{1}{2}}},$$

$$R_2 = 1 + \frac{R_2^*}{g\overline{\eta}_2^*} = 1 + \frac{R_1^*}{g\overline{\eta}_2^*} = 1 + \frac{(R_1-1)g\overline{\eta}_1^*}{g\overline{\eta}_2^*} \implies R_2 = 1 + \frac{R_1-1}{r}.$$

For the next non-dimensionalisations, the spatial discretisation is required, indicated by $j$, for $j = 1, 2, \ldots, N$. We will have

$$(B_j)_2 = \frac{(B_j^*)_2}{g\overline{\eta}_2^*} = \frac{(B_j^*)_1}{g\overline{\eta}_2^*} = \frac{(B_j^*)_1 g\overline{\eta}_1^*}{g\overline{\eta}_2^*} \implies (B_j)_2 = \frac{(B_j)_1}{r^{\frac{1}{2}}}.$$

As the origin of the system is at the water bottom, the non-dimensional form of the free surface elevation is expressed as

$$(\eta_j)_2 = 1 + \frac{(\eta_j^*)_2}{\overline{\eta}_2^*} = 1 + \frac{(\eta_j^*)_1}{\overline{\eta}_2^*} = 1 + \frac{[(\eta_j)_1 - 1]\overline{\eta}_1^*}{\overline{\eta}_2^*} \implies (\eta_j)_2 = 1 + \frac{(\eta_j)_1 - 1}{r}.$$

Yet, despite these remain constant, the non-dimensional energy flow and wave period are

$$F_2 = \frac{F_2^*}{\rho\,[g^3(\overline{\eta}_2^*)^5]^{\frac{1}{2}}} = \frac{F_1^*}{\rho\,[g^3(\overline{\eta}_2^*)^5]^{\frac{1}{2}}} = \frac{F_1\,\rho\,[g^3(\overline{\eta}_1^*)^5]^{\frac{1}{2}}}{\rho\,[g^3(\overline{\eta}_2^*)^5]^{\frac{1}{2}}} \implies F_2 = \frac{F_1}{r^{\frac{5}{2}}},$$

$$\tau_2 = \tau_2^*\left(\frac{g}{\overline{\eta}_2^*}\right)^{\frac{1}{2}} = \tau_1^*\left(\frac{g}{\overline{\eta}_2^*}\right)^{\frac{1}{2}} = \tau_1\left(\frac{g\overline{\eta}_1^*}{g\overline{\eta}_2^*}\right)^{\frac{1}{2}} \implies \tau_2 = \frac{\tau_1}{r^{\frac{1}{2}}}.$$

## 5. Results

On this section we will show the results obtained. These are organised in 10 cases on which we have experimental data for comparison. These cases, described in detail below, are referenced as waves 1 to 3 and from 4(a) to 4(g).

### 5.1. Comparison with experiments

For comparison with the experiments, we will use wave data obtained in beaches and in testing tanks. These experiments were originally related in Hansen e Svendsen [11] and in Eagleson [6] and were used in comparisons with other methods and theories. See, for example [14] and [16].

The experimental data were obtained from uniform beach slope of 1/35 [11] and from slope of 1/15 [6] in laboratory tanks. The data were collected until the wave breaking, point in which the modeling presented in this paper is no longer applicable.

| Wave | $H_0$ | $\tau_0$ | $H_0^*$ (mm) | $\tau_0^*$ (s) |
|---|---|---|---|---|
| 1 | 0,31 | 5,72 | 93 | 1 |
| 2 | 0,13 | 9,55 | 39 | 1,67 |
| 3 | 0,14 | 19,04 | 42 | 3,33 |

Table 1: Initial values of heights and periods for waves 1 to 3. Experimental data of Hansen e Svendsen [11].

For the first simulations we used the parameters $D = 1$, the number $N$ of terms for the Fourier's expansions in (11) and (12) equals to 16 and $r = 0,999$. In table 1, we summarised the cases of waves 1 to 3 which we are now going to examine with the simulations done with the present method.

In figures 1(a) and 1(b) we show, respectively, the wave height and its phase velocity as a function of depth, for wave 1. With non-dimensional values of the initial height and the initial period, given respectively, by $H_0 = 0,31$ and $\tau_0 = 5,72$, an excellent agreement between the simulation and the experimental data is visually observed, before the wave breaks.

Wave 2 is shorter and has a greater initial period. The comparison for this case is represented in figure 2.

In figure 3, similar comparisons are done for wave 3 which presents a significantly greater period than the former ones. Again, we observe that the simulations present a good agreement with the experimental data. Particularly, the shoaling of waves is remarkable, with the decrease of the depth, in all cases until values very close to the point of break of the wave.

In the following cases, we show the comparison with experimental data [6], obtained in a wave tank with uniform slope of 1/15. Seven simulations are reported, where the dimensional parameters that define them are in table 2. In this table it is also shown the values of initial waves steepness, which is given by $\varepsilon = \frac{H^*}{\lambda^*}$, according to Eagleson [6] and according to our numerical simulations. The reference level is $D = 1$ in all cases except in case (f), where $D = 0,9$. This difference is due to the wave height being a little smaller, in this case. The number of terms on the Fourier expansions used for the next simulations is $N = 32$.

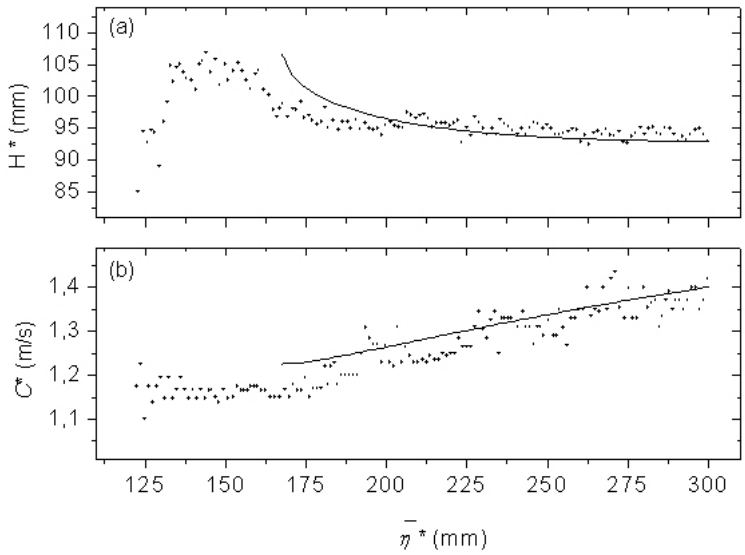


Figure 1: (a) Wave height as a function of water depth. (b) Phase velocity of the wave function of depth for wave 1. The solid line indicates the data obtained from numerical simulations with the present method and the points indicate the data obtained experimentally by [11].

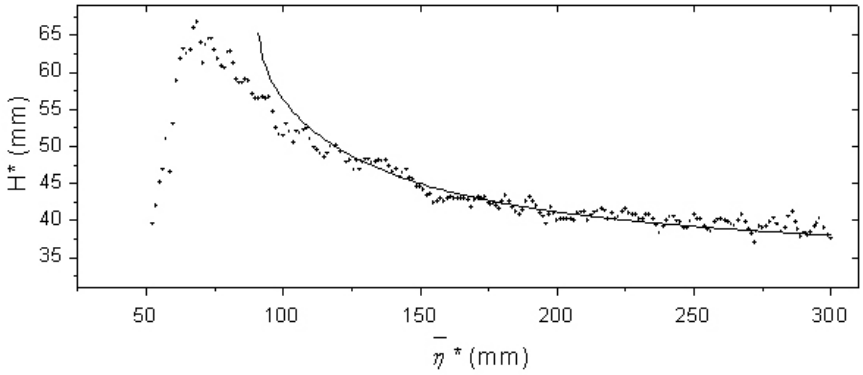


Figure 2: Wave height as a function of water depth for wave 2. The solid line indicates the data obtained from numerical simulations with the present method and the points indicate the data obtained experimentally by [11].

Figure 4 shows the wave shoaling coefficient, given by $\frac{H}{H_0}$, as a function of the respective relative water depth for waves 4(a) to 4(g). This coefficient represents only the relation of the wave height with the decrease of the depth, while the relative depth, indicates if the wave is in shallow, intermediate or deep waters. In all 7 cases, we had an intermediate water regime according to the ratio $0,05 > \frac{\overline{\eta}^*}{\lambda^*} < 0,5$. We observed on this regime a simulated shoaling very close to reality.

On next subsections we analyses with detail the height and the shape of the waves close to their break, using the computational tool we developed and validated here.

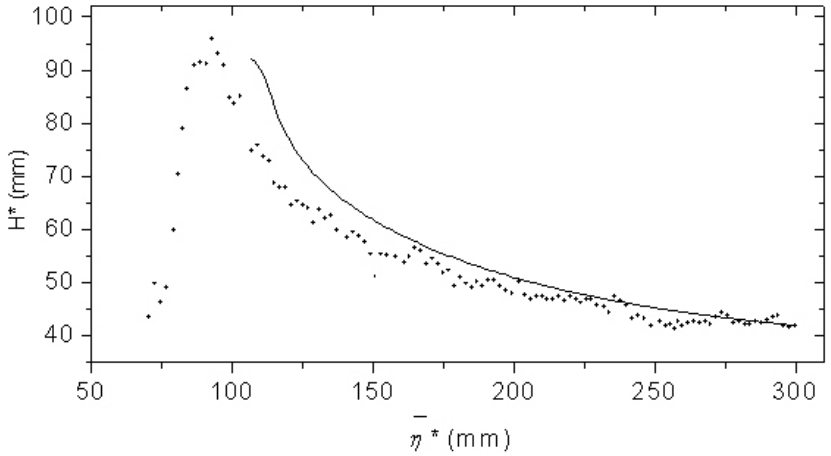


Figure 3: Wave height as a function of water depth for wave 3. The solid line indicates the data obtained from numerical simulations with the present method and the points indicate the data obtained experimentally by [11].

| Wave | $\overline{\eta}_0^*$ (feet) | $H_0^*$ (feet) | $\tau_0^*$ (s) | $H_0^*/\lambda_0^*$ (according to [6]) | $H_0^*/\lambda_0^*$ (simulated) |
|---|---|---|---|---|---|
| 4(a) | 1,75 | 0,230 | 0,938 | 0,0528 | 0,051739 |
| 4(b) | 1,75 | 0,234 | 1,101 | 0,0396 | 0,039545 |
| 4(c) | 1,75 | 0,357 | 1,105 | 0,0598 | 0,059963 |
| 4(d) | 1,75 | 0,440 | 1,235 | 0,0611 | 0,061695 |
| 4(e) | 1,75 | 0,354 | 1,389 | 0,0420 | 0,041634 |
| 4(f) | 1,75 | 0,186 | 1,428 | 0,0209 | 0,021037 |
| 4(g) | 1,75 | 0,265 | 1,684 | 0,0237 | 0,023999 |

Table 2: Initial values of water depth, the height, the period and the slope according to the experimental data of [6] and the slope calculated by the present method.

### 5.2. Breaking height

Waves propagating in the shoaling zone, in intermediate waters, become unstable and break when the velocity of the water particle on the wave crest becomes equal or greater than the phase velocity of the wave. At breaking, the wave height is limited by the depth and the wavelength. For a given depth and wave period, there is a maximum limit for the wave height, called *wave breaking height*. According to Stoke's theory, in intermediate waters, the breaking height is $\frac{H}{\overline{\eta}} = 0,78$ [15, p. 06].

In our model, $\eta(x)$ is by definition only defined for each $x$. Therefore, the method used for the solution will not apply until the physical limit of the wave break. Before the break, the wave surface becomes multivalued and thus not modelled by a function. In the specific case of Newton's method, it will diverge.

We defined as *computational wave breaking height* and denoted by $\left(\frac{H^*}{\overline{\eta}^*}\right)_b$, the

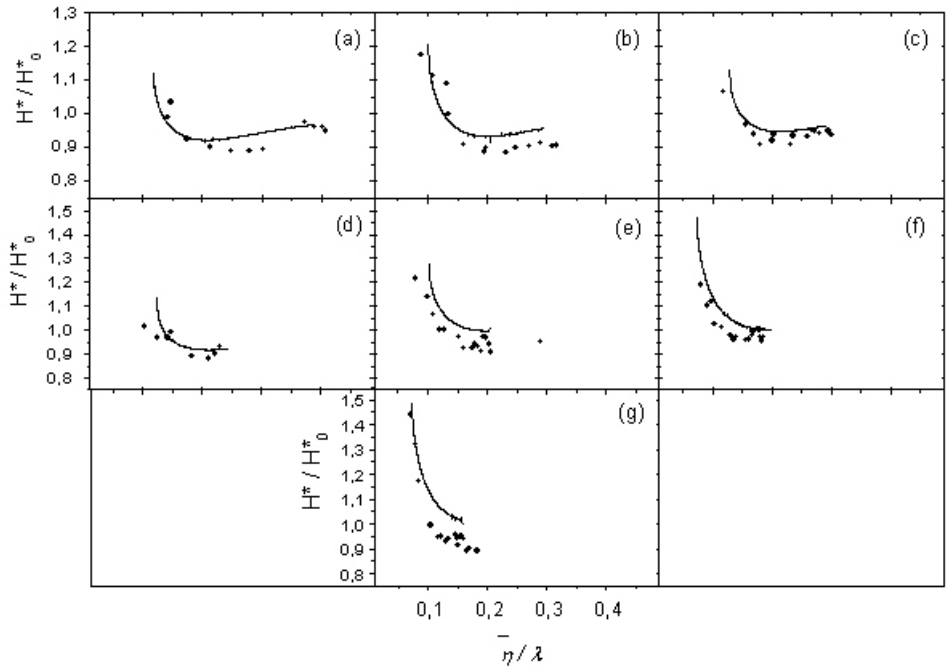


Figure 4: Wave's shoaling coefficient a function on the depth of water to the waves 4 (a) to 4 (g) (see table 2). The solid line indicates the data obtained from numerical simulations with the present method and the points indicate the data obtained experimentally by [6].

last height for which there has been convergence of Newton's method described in subsection 4.1.

Figure 5 shows the evolution of parameter height by depth, given by $H^*/\overline{\eta}^*$, the computation wave breaking height $\left(\frac{H^*}{\overline{\eta}^*}\right)_b$ as a function of parameter $\overline{\eta}/\lambda$, and the depth relative to the wavelength. In this figure, cases of waves 1, 2 and 3 are shown.

On curve 5(a) with height and initial period $H_0 = 0,31$ and $\tau_0 = 5,72$ respectively, the initial relative depth is $\frac{\overline{\eta}_0}{\lambda_0} = 0,214$ and the relative depth on the wave break is $\frac{\overline{\eta}}{\lambda} = 0,13256$. This indicates that the whole shoaling process until the break of the wave happened in intermediate waters.

On curve 5(b), representing wave 2, the initial relative depth is $\frac{\overline{\eta}_0}{\lambda_0} = 0,1128$ and the relative depth on the wave break is $\frac{\overline{\eta}}{\lambda} = 0,0516$. This wave also had the process of shoaling and breaking in intermediate waters, but it breaks practically in shallow waters and with a greater height.

The wave represented on curve 5(c) is significantly longer and presents practically all of its shoaling process in shallow waters, breaking with $\left(\frac{H^*}{\overline{\eta}^*}\right)_b = 0,755$ on a relative depth of $\frac{\overline{\eta}}{\lambda} \approx 0,027$. We observed that the model and the computational method predict a breaking height very close to the observed experimentally.

The cases referred to waves 4(a) to 4(g) on table 2 are represented and summarised

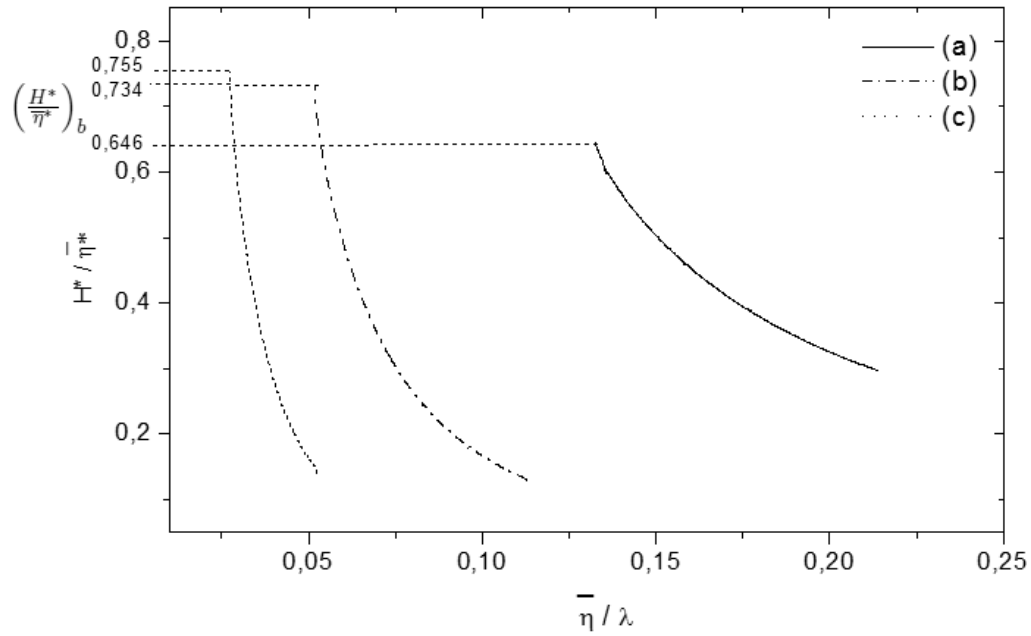


Figure 5: The evolution of the parameter $H^*/\overline{\eta}^*$ and computational wave's breaking height, $\left(\frac{H^*}{\overline{\eta}^*}\right)_b$ a function of depth relative to the wavelength, $\overline{\eta}/\lambda$. In figure $(a)$, we show the results referring to figure 1, in figure $(b)$, referring to figure 2 e in figure $(c)$, referring to figure 3.

in figure 6. We can verify that all the shoaling processes until the break of the waves, occur in intermediate waters. Furthermore, we see that the computational breaking heights are so that $\frac{H}{\overline{\eta}} \approx 0,7$. This is a value that reaffirms the good performance of the method to model the phenomenon of wave shoaling.

### 5.3. Waves profile and their breaking angles

By using Stokes theory, it can be shown [12] that the breaking angle of a wave is 120°. We are going to use the spectral method described in this paper to estimate the *computational breaking angle* $\alpha$, i.e., the one until when we can obtain convergence of Newton's method used for solving the system of nonlinear equations which governs the water waves.

Figures 7 to 9 represent the cases of waves 1 to 3, respectively.

Figures are double: part (I) shows the wave profile on the initial instant and part (II), at the moment of the computational wave break. A horizontal straight line is included in all figures to represent the average depth. To estimate the value $\alpha$, we used a straight line passing by three points next to the crest, using symmetry, and calculated the line's angular coefficient.

It can be verified that the way the wave shoals depends directly on the wavelength. For waves of greater length, we note that the wave's trough becomes horizontally longer. With this, the crest has a more pronounced increase on the wavelength.

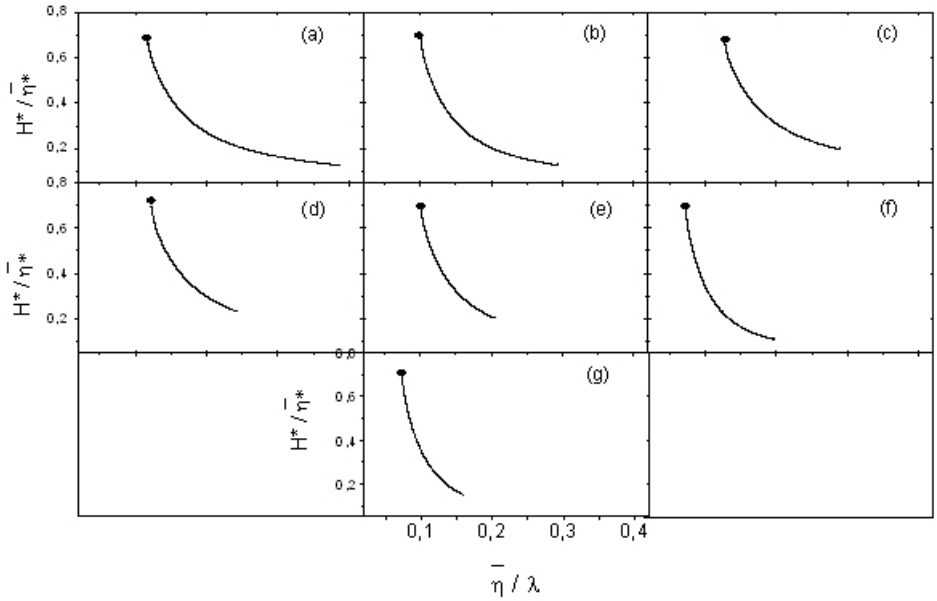


Figure 6: The evolution of the parameter $H^*/\overline{\eta}^*$ and computational wave's breaking height, $\left(\frac{H^*}{\overline{\eta}^*}\right)_b$ a function of the relative depth of water referring to initial data contained in table 2 and also shown in figure 4.

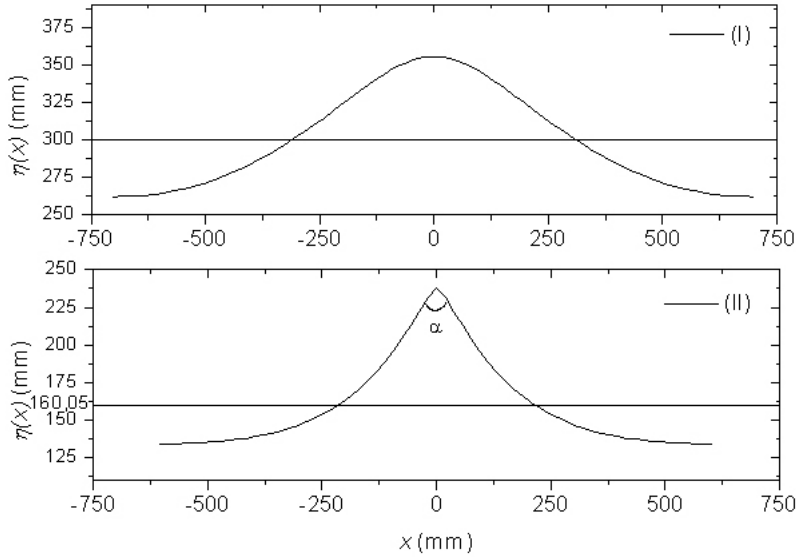


Figure 7: Wave profile: The figure (I) shows the wave profile at the initial moment, with $\overline{\eta}_0^* = 300$ mm, $H_0^* = 93$ mm and $\tau_0^* = 1,0$ s. The figure (II) shows the wave profile at the moment of the break, In this case, the depth of water is indicated by straight line $\overline{\eta}^* = 160,05$ mm.

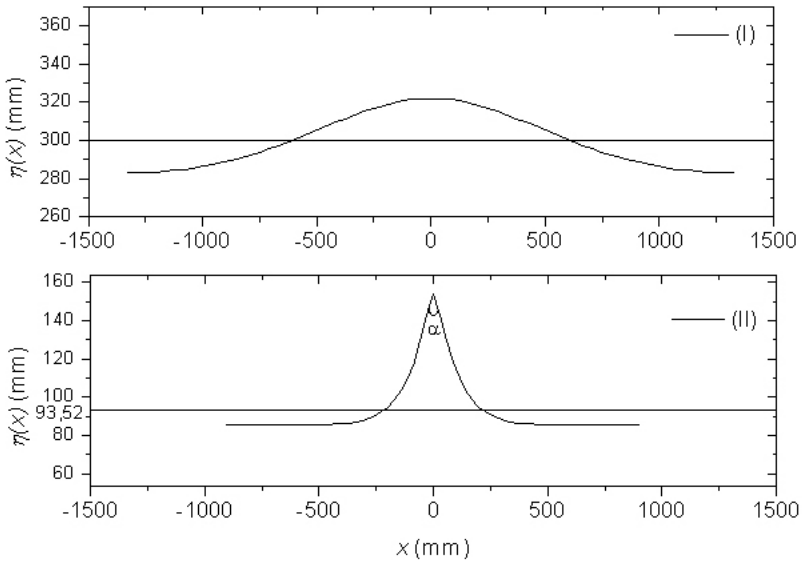


Figure 8: Wave profile: Figure (I) shows the wave profile at the initial moment, with $\overline{\eta}_0^* = 300$ mm, $H_0^* = 39$ mm and $\tau_0^* = 1,67$ s. The figure (II) shows the wave profile at the moment of breaking, In this case, the depth of water is indicated by straight line is $\overline{\eta}^* = 93,52$ mm.

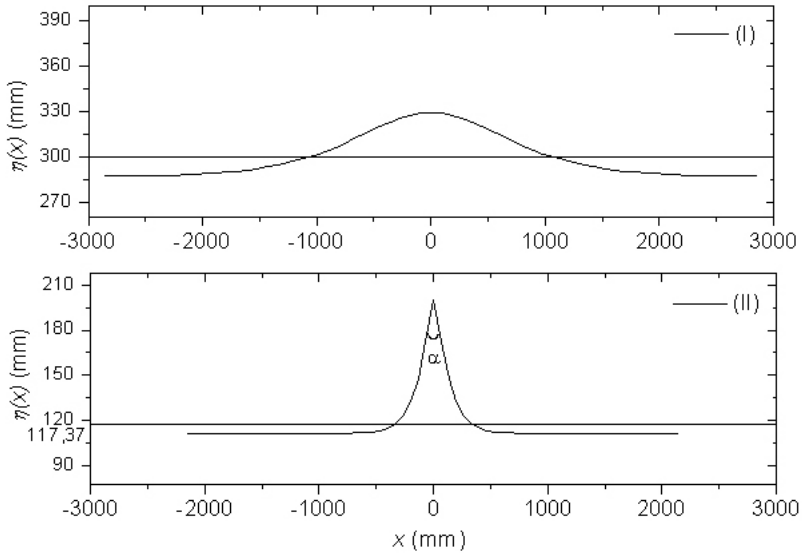


Figure 9: Wave profile: Figure (I) shows the wave profile at the initial moment, with $\overline{\eta}_0^* = 300$ mm, $H_0^* = 42$ mm and $\tau_0^* = 3,33$ s. The figure (II) shows the wave profile at the moment of breaking, In this case, the depth of water is indicated by straight line is $\overline{\eta}^* = 117,37$ mm.

We can observe that the computational breaking angles of waves 1, 2 and 3 were $134,12°, 142,64°$ and $126,20°$ respectively. The first two are in intermediate waters, while wave 3, which propagates in shallow waters, has the smaller breaking angle.

We then revisited the cases of waves 4(a)-4(g), presented in subsection 5.1 and showed at table 2. Table 3 shows the heights and periods of waves at the initial moment, apart from the water depths and computational breaking angles. The initial depth is equal to $\overline{\eta}_0^* = 1,75$ feet, in all cases.

| Wave | $H_0^*$ (feet) | $\tau_0^*$ (s) | $\overline{\eta}_f^*$(feet) | $\alpha$ (degrees) |
|---|---|---|---|---|
| 4(a) | 0,230 | 0,938 | 0,3817 | 124,14 |
| 4(b) | 0,234 | 1,101 | 0,4110 | 123,60 |
| 4(c) | 0,357 | 1,105 | 0.6066 | 122,48 |
| 4(d) | 0,440 | 1,235 | 0,7140 | 119,30 |
| 4(e) | 0,354 | 1,389 | 0,6591 | 124,48 |
| 4(f) | 0,186 | 1,428 | 0,3989 | 130,49 |
| 4(g) | 0,265 | 1,684 | 0,5644 | 128,58 |

Table 3: Data for the wave profiles. The values of the initial heights and initial wave periods as well as the water depths and angles formed on the crests of the waves at the moment when they break.

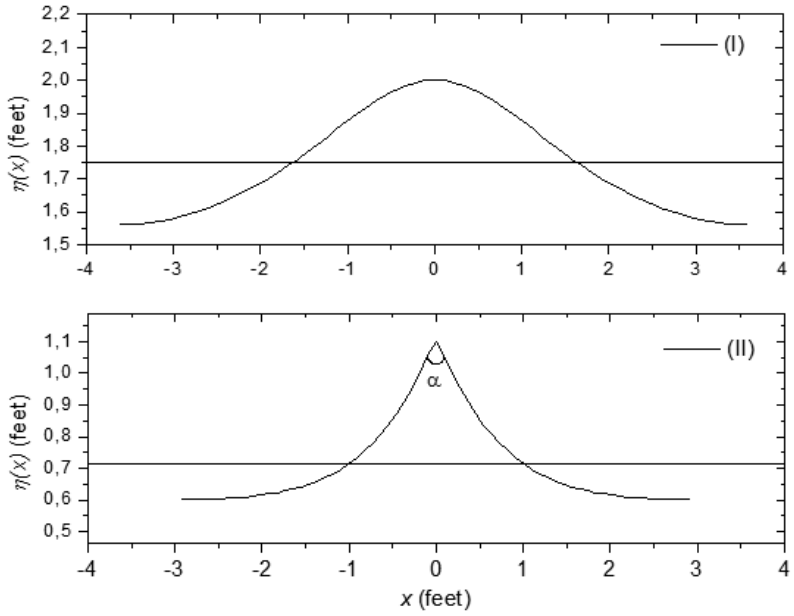


Figure 10: Profile of waves of the case (d) of table 3: Figure (I) shows the wave profile at the initial moment and the figure (II) shows the wave profile at the moment of the break.

To calculate the breaking angles in all cases given at table 3, tree points subsequent to the wave crest were used. We notice that all breaking angles were practically identical and slightly greater than the limit for the breaking angle given in the literature.

Figure 10 shows the profile of the waves of case 4(d) at table 3. The remaining cases have a similar graphical aspect.

Thus as waves 1, 2 and 3, waves 4(a)-4(g) present a common characteristic of shoaling which is the decrease in the wavelength and an increase in its height, with the trough becoming horizontally longer. This is the eminent and favourable aspect to the wave break.

## 6. Conclusion

A Fourier approximation method was employed for modeling and simulating fully nonlinear steady water waves. The resulting set of nonlinear equations was solved by Newton's method. After a careful non-dimensionality, we assumed that in an inclined bottom, the waves, in any depth, behave as in horizontal bottoms. An iterative method was described for the study of wave shoaling.

A set of experimental data was used to define the initial states in 10 study cases. From those, we could validate the method which presented excellent agreement with the measurements. An analysis of the so called wave breaking height and computational breaking angle was done and values were obtained for comparison between simulations and the theoretical criteria of breaking height and angle. These results, therefore contribute to the knowledge of existing relationships between analytical-computational approximation methods and the theory of nonlinear surface waves.

## Acknowledgements

The first author carried out part of work with a grant by CAPES and the second author, as a member of the EU project FP7-295217 - HPC-GA. His research was supported by Grant MTM2011-24766 of the MICINN, Spain and also by the Basque Government through the BERC 2014-2017 program and by Spanish Ministry of Economy and Competitiveness MINECO: BCAM Severo Ochoa excellence accreditation SEV-2013-0323.

## References

[1] Bingham, H. and Zhang, H.: On the accuracy of finite-difference solutions for nonlinear water waves. J. of Engng Math. **58**, (2007), 211–228.

[2] Burden, R. L. and Faires, J. D.: *Numerical analysis*. Brooks-Cole Publishing, 2004.

[3] Dommermuth, D. G. and Yue, D. K. P.: A high-order spectral method for the study of nonlinear gravity waves. J. Fluid Mech. **184** (1987), 267–288.

[4] Drimer, N. and Agnon, Y.: An improved low-order bounday element method for breaking surface waves. Journal of Wave Motion **43** (2006), 241–258.

[5] Ducrozet, G., Bingham, H. B., Engsig-Karup, A. P., Bonnefoy, F., and Ferrant, P.: A comparative study of two fast nonlinear free-surface water waves models. Int. J. Num. Methods in Fluids **69** (2012), 1818–1834.

[6] Eagleson, P. S.: Properties of shoaling waves by theory and experiment. Transactions, American Geophysical Union **37** (1956), 565–572.

[7] Fenton, J. D.: A fifth-order Stokes theory for stead waves. J. Waterway, Port, Coastal, Ocean Engng. **111** (1985), 216–234.

[8] Fenton, J. D.: The numerical solution of stedy water wave problems. Computers and Geosciences **14** (3) (1988), 357–368.

[9] Freilich, M. H. and Guza, R. T.: Nonlinear effects on shoaling surface gravity waves. Phil. Trans. R. Soc. Lond. A **311** (1984), 1–41.

[10] Giménez-Curto, L. A. and Corniero Lera, M. A.: Application of Fourier methods to water waves in small depths. Applied Ocean Res. **18** (1995), 275–281.

[11] Hansen, J. B. and Svendsen, I. A.: Regular wave in shoaling water: experimental data. *Inst. of Hydrodynamics and Hydraulic Engng. Tech. Univ. of Denmark*, series paper No. 21 , 1979.

[12] Kinsman, B.: *Wind waves - their generation and propagation on the ocean surface*. Prentice-Hall, Inc.: New Jersey, 1965.

[13] Pihl, J. H., Bredmose H., and Larsen, J.: Shoaling of sixth-order waves on a current. Ocean Engng. **28** (2001), 667–687.

[14] Rienecker, M. M. and Fenton, J. D.: A Fourier approximation method for steady water waves. J. Fluid Mech. **104** (1981), 119–137.

[15] Secretariat of the World Meteorological Organization. Guide to Wave Analysis and Forecasting, No. 702, Geneva, Switzerland, 1998.

[16] Stiassnie, M. and Peregrine, D. H.: Shoaling of finite-amplitude surface waves on water of slowly-varying depth. J. Fluid Mech. **97** (1980), 783–805.

[17] Tsai, C., Chen, H., Hwung, H., and Huang, M.: Examination of empirical formulas for wave shoaling and braking on steep slopes. Ocean Engineering **32** (2005), 469–483.

[18] Tsai, W. and Yue, D. K. P.: Computation of nonlinear free-surface flows. Annual Reviews Fluids Mechanic **28** (1996), 249–278.

[19] Whitham, G. B.: *Linear and nonlinear waves*. John Wiley, New York, 1974.